ARTICLE
Journal of Cellular Biochemistry 112:2574–2584 (2011)

Journal of Cellular Biochemistry

EBP50 Is Involved in the Regulation of Vascular Smooth Muscle Cell Migration and Cytokinesis

Nicolas Baeyens,[1] Carole de Meester,[2] Xavier Yerna,[1] and Nicole Morel[1]*

[1]*Laboratory of Cell Physiology, Institute of Neuroscience, Université Catholique de Louvain, Avenue Hippocrate 55, 1200 Brussels, Belgium*

[2]*Division of Cardiology, Institut de Recherche Expérimentale et Clinique, Université Catholique de Louvain, Avenue Hippocrate 55, 1200 Brussels, Belgium*

ABSTRACT

Ezrin, Radixin, Moesin binding phosphoprotein 50 (EBP50) is a scaffold protein that possesses two PDZ interacting domains. We have shown that, in isolated artery stimulated with noradrenaline, EBP50 interacts with several elements of the cytoskeleton. However, the contribution of EBP50 to the organization of the cytoskeleton is unknown. We have used primary cultured vascular smooth muscle cells to investigate the involvement of EBP50 in the regulation of cell architecture, motility and cell cycle, and to identify its target proteins and subsequent action mechanism. The results showed that depletion of EBP50 by siRNA transfection induced changes in cell architecture and increased cell migration. The same phenotype was induced by inhibition of myosin IIa and this effect was not additive in cells depleted for EBP50. Moreover, a larger proportion of binucleated cells was observed after EBP50 depletion, indicating a defect in cytokinesis. The identification, after co-immunoprecipitation, of a direct interaction of EBP50 with both tubulin and myosin IIa suggested that EBP50 could regulate cell migration and cytokinesis by linking myosin IIa fibers and microtubule network. Indeed, depletion of EBP50 also dismantled myosin IIa fibers and induced the formation of stable microtubules in lamellae expansions and Rac1 activation. This signaling cascade leads to the formation of lamellipodia, trailing tails and decrease of focal adhesion formation, triggering cell migration. J. Cell. Biochem. 112: 2574–2584, 2011.

KEY WORDS: EBP50; MIGRATION; CYTOKINESIS; MYOSIN IIA; VASCULAR SMOOTH MUSCLE

Vascular smooth muscle cells (VSMC) in the arterial wall are characterized by a contractile, non-proliferating and non-migratory phenotype. During vascular development in response to growth factors, and in response to various stimuli like mechanical stress, vascular injury or inflammation, VSMC undergo a change to a migratory and proliferative phenotype [Gerthoffer, 2007]. Several components of the cell cytoskeleton are involved in triggering cell migration: on one hand, acto-myosin and focal adhesions [Gardel et al., 2008; Pasapera et al., 2010], and, on the other hand, microtubules [Waterman-Storer et al., 1999; Etienne-Manneville and Hall, 2002], forming dynamic interacting networks regulated by multiple associated proteins.

We have shown that, in noradrenaline-stimulated rat mesenteric arteries, Ezrin, Radixin, Moesin binding phosphoprotein 50 (EBP50) interacts with several components of the non-contractile cytoskeleton and modulates the contractile properties of the artery [Baeyens et al., 2010], suggesting that this protein could be an important regulator of the cytoskeleton. EBP50 is a scaffold protein containing two different PDZ domains and a C terminal sequence that binds to the N terminal FERM domain of Ezrin, Radixin, and Moesin proteins (ERM) [Reczek et al., 1997]. EBP50 is mainly reported to interact with membrane proteins such as CFTR, β_2-receptor, or NHE3 [Weinman et al., 1995; Short et al., 1998; Cao et al., 1999]. This protein is also known under the name of NHERF1, due to its interaction with the NHE exchanger.

Recently, depletion of EBP50 has been reported to decrease the F-actin content in human bronchial epithelial cells [Favia et al., 2010] and to cause a strong defect in epithelium microvilli formation, a structure enriched in ezrin and acto-myosin and anchored to a myosin II terminal web [Garbett et al., 2010].

Additional Supporting Information may be found in the online version of this article.

Grant sponsor: Ministère de l'Education et de la Recherche Scientifique of the Belgian French Community; Grant number: ARC06/11-339; Grant sponsor: Fonds pour la Recherche Scientifique Médicale (Belgian French Community).

*Correspondence to: Prof. Nicole Morel, SSS/IONS Pasteur, Avenue Mounier 53 Bte B1.53.03, 1200 Bruxelles, Belgium. E-mail: nicole.morel@uclouvain.be

Received 4 May 2011; Accepted 9 May 2011 • DOI 10.1002/jcb.23183 • © 2011 Wiley-Liss, Inc.
Published online 19 May 2011 in Wiley Online Library (wileyonlinelibrary.com).

Moreover, Sip1, the *Drosophila* ortholog of EBP50, is involved in adherens junction and actin architecture stabilization [Hughes et al., 2010], in agreement with a role for EBP50 in cytoskeleton modulation. In addition, EBP50 is over-expressed in injured arteries, indicating that EBP50 could play an important role in vascular pathologies [Song et al., 2010].

In a previous study, we have identified the binding of EBP50 to tubulin and to myosin IIa in noradrenaline-stimulated rat mesenteric artery [Baeyens et al., 2010]. Recent studies have highlighted the inhibitory role of non-muscular myosin IIa in migration. Inhibition of myosin IIa evokes a marked increase in cell migration associated with the formation of lamellipodia and filopodia, microtubule stabilization in the lamellipodia and the activation of the small Rho-GTPase Rac1 [Katsumi et al., 2002; Even-Ram et al., 2007; Lee et al., 2010]. The contractile tension mediated by myosin and its actin cross-linking activity act synergistically to promote the formation of actin filaments bundles and the maturation of focal adhesions [Choi et al., 2008]. These results indicate that myosin IIa is required for the maintenance of the equilibrium between the acto-myosin and microtubule networks that controls cell motility.

These observations led us to further investigate the involvement of EBP50 in cytoskeleton modulation, and the mechanism of EBP50 contribution to cell migration and cell cycle regulation in migratory, proliferative primary VSMC obtained from rat aorta. EBP50 expression was inhibited by transfection of a specific siRNA. The results indicate that EBP50 is involved in the control of VSMC migration and cytokinesis through a myosin IIa-dependent mechanism.

MATERIALS AND METHODS

CELL CULTURE AND REAGENTS

Male Wistar rats (150–200 g) were anesthetized with diethyl ether and killed by decapitation in accordance with international guidelines and with the approval of the local ethic committee for animal experiments.

Rat aorta was cleaned from adherent tissue, and endothelium denuded. Pieces of aorta (2 mm^2) were cultured in Dulbecco's modified Eagle's medium (DMEM) supplemented with 10% fetal bovine serum (FBS), penicillin, streptomycin, and 2 mM glutamine in an incubator at 37°C with humidified 5% CO_2. Cells migrated from the pieces of aorta after 2–3 days. Aortic pieces were then removed and VSMC were left to proliferate. They were used between the third and the sixth passage.

Vinblastine, inhibitor of microtubule polymerization was purchased from Sigma–Aldrich. Blebbistatin, inhibitor of myosin II was purchased from Tocris Bioscience.

siRNA TRANSFECTION

Cells were cultured in DMEM supplemented with FBS 10% and without antibiotics for 24 h and then transfected with 5 nM siRNA (Stealth siRNA, Invitrogen) by using RNAiMAX Lipofectamine, following manufacturer's instructions (Invitrogen). Sequence for each siRNA was:

EBP50 siRNA (1): GACAAGGAAACAGAUGAGUUCUUUA & UAAAGAACUCAUCUGUUUCCUUGUC.

EBP50 siRNA (2): GAGAAAGGCAAGGUGGGCCAGUUUA & UAAACUGGCCCACCUUGCCUUUCUC.

Myosin IIa siRNA: AAAUGUGGAAGGUUCUUUCCUCCUU & AAGGAGGAAAGAACCUUCCACAUUU.

Cells were cultured for 96 h to allow a maximal inhibition of protein expression. Knock-down efficiency was assessed by Western blotting. Proteins were extracted with a non-denaturating extraction buffer: Igepal CA-630 0.5%, dithiothreitol 1 mM, Hepes 50 mM (pH 7.6), and Halt protease/phosphatase 1% (ThermoFischer). Protein concentration was determined by the BCA (bicinchoninic acid) method (Thermoscientific). For myosin IIa, a better extraction was achieved with a denaturating buffer containing urea 9.5 M, Igepal CA-630 2%, β-mercaptoethanol 5%, pharmalytes (pI: 3-10) 1%, Halt proteases/phosphatases 1% (Thermoscientific). Proteins were resolved by SDS–PAGE (NuPAGE 4–12% MOPS, Invitrogen) and blotted onto PVDF membrane (iBlot, Invitrogen). Membranes were probed with anti-nherf1 (1/1,000, Sigma) or anti-myosin IIa (1/1,000, Cell Signaling) antibodies and anti-actin (1/1,000, Santa Cruz) antibody as loading control. IRDye conjugated fluorescent secondary antibodies (680 and 800 nm) were used to detect primary antibodies. Bands were detected and quantified with an Odyssey infrared imaging system (Li-Cor).

MICROSCOPY

Cells grown on glass coverslips were washed with PBS, fixed with 4% PFA for 10 min and permeabilized with Triton 0.5% for 5 min (F-actin visualization kit, Cytoskeleton). Cells stained for tubulin were fixed with cold methanol 100% for 5 min at −20°C. Cells were incubated for 1 h with StartingBlock blocking buffer (Thermoscientific) and stained with primary antibodies of interest: anti-nherf1 (1/200, Sigma), anti-myosin IIa (1/200, Cell Signaling), anti-vinculin (1/200, Sigma), anti-tubulin (1/400, Cytoskeleton), or rhodamine-phalloïdin (20 nM, F-actin visualization kit, Cytoskeleton) and thereafter probed with the corresponding secondary antibodies: Alexa 488- or 594-labeled donkey anti-rabbit, -mouse, or -sheep antibodies (Invitrogen). Cells were mounted on the coverslips with Prolong Gold antifade reagent (Invitrogen) and nuclei were stained with DAPI. Cells were observed with a Zeiss Axiovert S-100 microscope (Carl Zeiss, Inc) and individual images were acquired with a Zeiss Axiocam camera and a 20× objective (Zeiss Fluar, 0.75 NA) at room temperature. Images were analyzed with ImageJ software, background signal was reduced using the "subtract background" tool (ball radius: 100–200 pixels).

CELL MIGRATION

Cells were transfected with corresponding siRNA and grown to confluence for 96 h. FBS was removed from the culture medium 24 h before experiment. Cell layer was scratched with a sterile pipette tip. Cells were fixed and colored with hemalun–eosin staining solution after 0, 18, or 24 h of culture in FBS-free DMEM culture medium. Scratch line was imaged with a 4× objective (Zeiss Achroplan, 0.10 NA) at room temperature. Image analysis and estimation of the

refilling of the wound were done using the software Tscratch (CSE Laboratory, ETH Zurich, Switzerland) [Geback et al., 2009].

CO-IMMUNOPRECIPITATION

Proteins were extracted with the non-denaturating extraction buffer. Protein concentration was determined by the BCA method. Co-immunoprecipitation was performed as described [Baeyens et al., 2010]. Membranes were probed with anti-myosin IIa (Cell Signaling) or anti-tubulin antibodies (Cytoskeleton) (1/1,000). Bands were detected as described above. Controls with protein extract incubated with protein A sepharose without antibody and antibody bound to protein A sepharose incubated without protein extract were included.

PHOSPHORYLATION ANALYSIS

Proteins were extracted with the non-denaturating buffer. Protein concentration was determined by the BCA method. Protein extracts were resolved by SDS–PAGE and blotted onto PVDF membrane as described above. Membranes were probed with anti-MLC_{20} (Cell Signaling), anti-phospho MLC_{20} (Sigma), anti-actin (Santa Cruz), anti-Akt (Cell Signaling), and anti-phospho Akt (Cell Signaling) at a 1/2,000 concentration and were detected with Odissey infrared Imaging system as described above. Protein expression was normalized to actin level.

CELL CYCLE ANALYSIS

To perform cell cycle analysis, cells transfected for 96 h either with scramble or EBP50 siRNA were trypsinized, centrifuged, and incubated with a PSS solution containing 20 μg/ml propidium iodide (Sigma), 0.1% Triton, and 200 μg/ml RNAseA (Sigma). Cells were analyzed on a FACScan (Becton Dickinson) flow cytometer. Data were analyzed with FlowJo software.

Rac1-GTP G-LISA

For measurement of Rac1 activation, the Rac G-Lisa Activation Assay Biochem kit (Cytoskeleton) was used according to the manufacturer's recommendations. Total Rac1 protein level was measured by Western blot analysis with Rac1 antibody (Cytoskeleton) and normalized to the expression of actin.

DATA ANALYSIS

Data are expressed as mean ± SEM from at least three determinations. Statistical analysis was made using a two-way ANOVA with a Bonferroni post-test or by using a non-paired *t*-test to evaluate treatment differences (Prism, GraphPad software). $P < 0.05$ was considered to be significant.

RESULTS

EBP50 DEPLETION INDUCES STRUCTURAL CHANGES IN VASCULAR SMOOTH MUSCLE CELL ARCHITECTURE

Immunostaining of EBP50 in primary cultured VSMC revealed the distribution of this protein along thick filaments crossing the entire cell (Fig. 1A). The pattern of distribution was similar to that of actin (Fig. 1C). This localization suggests that EBP50 could interact with actomyosin bundles. In order to study the involvement of EBP50 in the modulation of the cell cytoskeleton, we transfected VSMC with two different siRNAs targeting EBP50. Controls were transfected with a scramble siRNA. After 96 h of culture, EBP50 protein expression was inhibited by 99 ± 0.5% and 97 ± 0.5% (n = 6), after transfection with the first and second anti-EBP50 siRNA, respectively (Fig. 1B). The inhibition was lower when cells were cultured for less than 96 h after transfection (EBP50 expression was inhibited by 54%, 87%, and 94% at 24, 48 and 72 h, respectively, after siRNA transfection).

Cells transfected with a scramble siRNA contained a central nucleus and numerous thick actin bundles (Fig. 1C). They seemed to develop a strong social behavior with many cell–cell interactions. Vinculin staining showed the presence of large focal adhesions all over the cell, and microtubules spread uniformly over the cell from the perinuclear region. Depletion in EBP50 drastically changed the cell morphology (Fig. 1C). Actin bundles were disassembled and cells formed lamellipodia and elongated trailing tails. The nuclei were rejected at cell periphery. Cells appeared isolated, and cell–cell interactions were suppressed. The area and the number of focal adhesions markedly decreased. Microtubule tubulin staining was prominent in membrane lamellae projections and weaker around the nucleus. Two different siRNAs directed against EBP50 were used and induced similar changes in cell architecture.

CELLS DEPLETED IN EBP50 DEVELOP MIGRATORY PROPERTIES AND PRESENT A DEFECT IN CYTOKINESIS

We assessed the migratory properties of VSMC by a wound healing test. In serum-free medium and in the absence of any stimulation, cells transfected with a scramble siRNA exhibited a constitutive ability to migrate and to refill the wound (Fig. 2A). By comparison, cells transfected with a siRNA directed against EBP50 were able to refill the wound more rapidly, showing faster migration rate than control cells. The two anti-EBP50 siRNA produced a similar increase in cell migration, dismissing the possibility of an off-target effect (Fig. 2A).

DAPI staining of the nuclei revealed an increase in the proportion of binucleated cells among EBP50-depleted cells compared to control cells (Fig. 2B). Only 5 ± 1% of binucleated cells were observed in cultures of cells transfected with scramble siRNA, while 19 ± 0.5% and 21 ± 1% of binucleated cells were observed in cultures of cells transfected with the first and second siRNA against EBP50, respectively (n = 4, $P < 0.05$ vs. control). No abnormal mitotic cells or apoptotic cells were observed. The data obtained by counting binucleated cells were confirmed by estimating the cell DNA content. FACS analysis of propidium iodide stained nuclei indicated that 6 ± 0.5% of control cells and 16 ± 2% of the cells transfected with EBP50-targeted siRNA were in G2/M phase (n = 3, $P < 0.05$; Fig. 2C), suggesting that EBP50 is a key player in cytokinesis.

DEPLETION OF MYOSIN IIa SHARES SIMILAR STRUCTURAL CHANGES WITH EBP50 DEPLETION IN VASCULAR SMOOTH MUSCLE CELLS

In a previous study, we identified myosin IIa as a partner of EBP50 in noradrenaline-stimulated arteries [Baeyens et al., 2010]. To confirm this observation in VSMC, we first determined the expression and

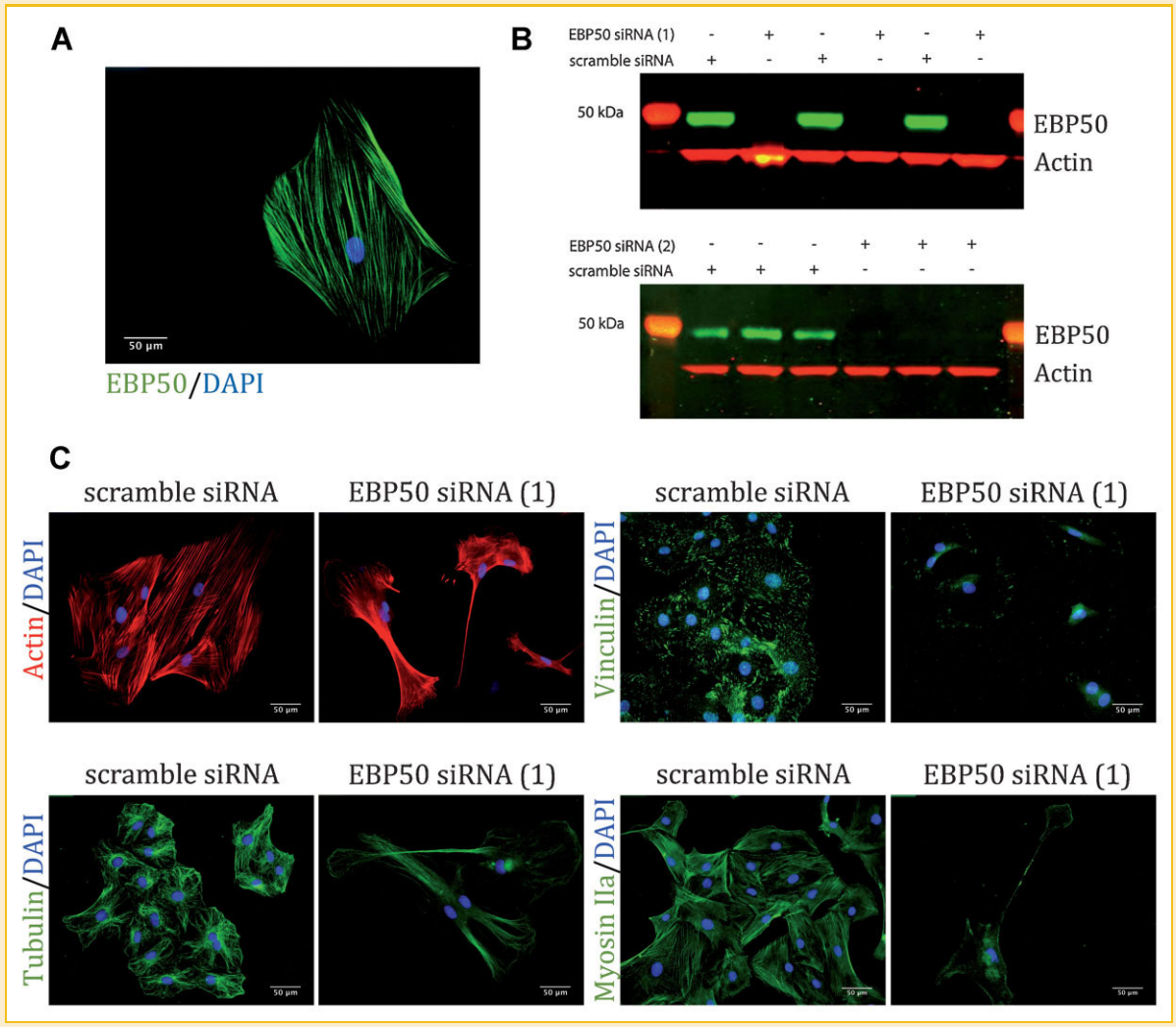

Fig. 1. Knock-down of EBP50 alters vascular smooth muscle cell architecture. A: Immunostaining of EBP50 (green) in primary VSMC. The nuclei were stained with DAPI (blue). B: Western blot of protein extracts from cells transfected either with a scramble siRNA or two different anti-EBP50 siRNA (5 nM). Membrane was immunoblotted with antibodies against EBP50 and actin, used as loading control and IRDye conjugated secondary antibodies (680 nm for actin in red and 800 nm for EBP50 in green). Signals were visualized and analyzed with an Odyssey infrared imager. After 96 h of culture, EBP50 protein expression was inhibited by 99 ± 0.5% with EBP50 siRNA #1 and 97 ± 0.5% with EBP50 siRNA #2 (mean ± SEM, n = 6). C: Representative images of VSMC stained for F-actin (phalloidin), focal adhesions with anti-vinculin antibody, tubulin (anti-α and -β tubulin) and myosin IIa after transfection of scramble or anti-EBP50 siRNA. Nuclei were stained with DAPI. Scale bars: 50 µm.

the localization of myosin IIa in VSMC by immunolabeling. Figure 3A illustrates the localization of myosin IIa in actin-based thick filaments, showing the same pattern of localization as EBP50. Knock-down of myosin IIa by specific siRNA transfection produced 98 ± 1% inhibition of myosin IIa expression after 96 h of culture (Fig. 3B). Two different bands were identified after Western blotting with anti-myosin IIa antibody: one at 140 kDa and the second at 230 kDa. Both bands disappeared after transfection of the myosin IIa-targeted siRNA, suggesting the existence of an alternative spliced variant of myosin IIa in rat VSMC. Depletion of myosin IIa in VSMC strongly affected actin bundles and cell architecture (Fig. 3C), in agreement with previous reports in other cell types [Even-Ram et al., 2007; Pasapera et al., 2010]. Lamellae with trailing tails appeared in myosin IIa-depleted cells. Nuclei were rejected towards the cell periphery and cell–cell interactions disappeared. The area and the number of focal adhesions decreased. Moreover, cells depleted for myosin IIa exhibited microtubule expansions into lamellae. This phenotype was similar to that of EBP50-depleted VSMC. EBP50 immunostaining in cells depleted in myosin IIa revealed a partial disorganization that could be related to the disruption of actin bundles (Fig. 3C).

EBP50 INTERACTS WITH MYOSIN IIa AND IS INVOLVED IN THE ALTERATION OF CELL MIGRATION INDUCED BY THE INHIBITION OF MYOSIN IIa IN VASCULAR SMOOTH MUSCLE CELL

To explain the similarity of the effects of myosin IIa and EBP50 depletion in VSMC, we investigated the potential interaction between the two proteins by co-immunoprecipitation (Fig. 4A). Western blot analysis of the proteins immunoprecipitated by an anti-EBP50 antibody revealed a large band at 230 kDa, after

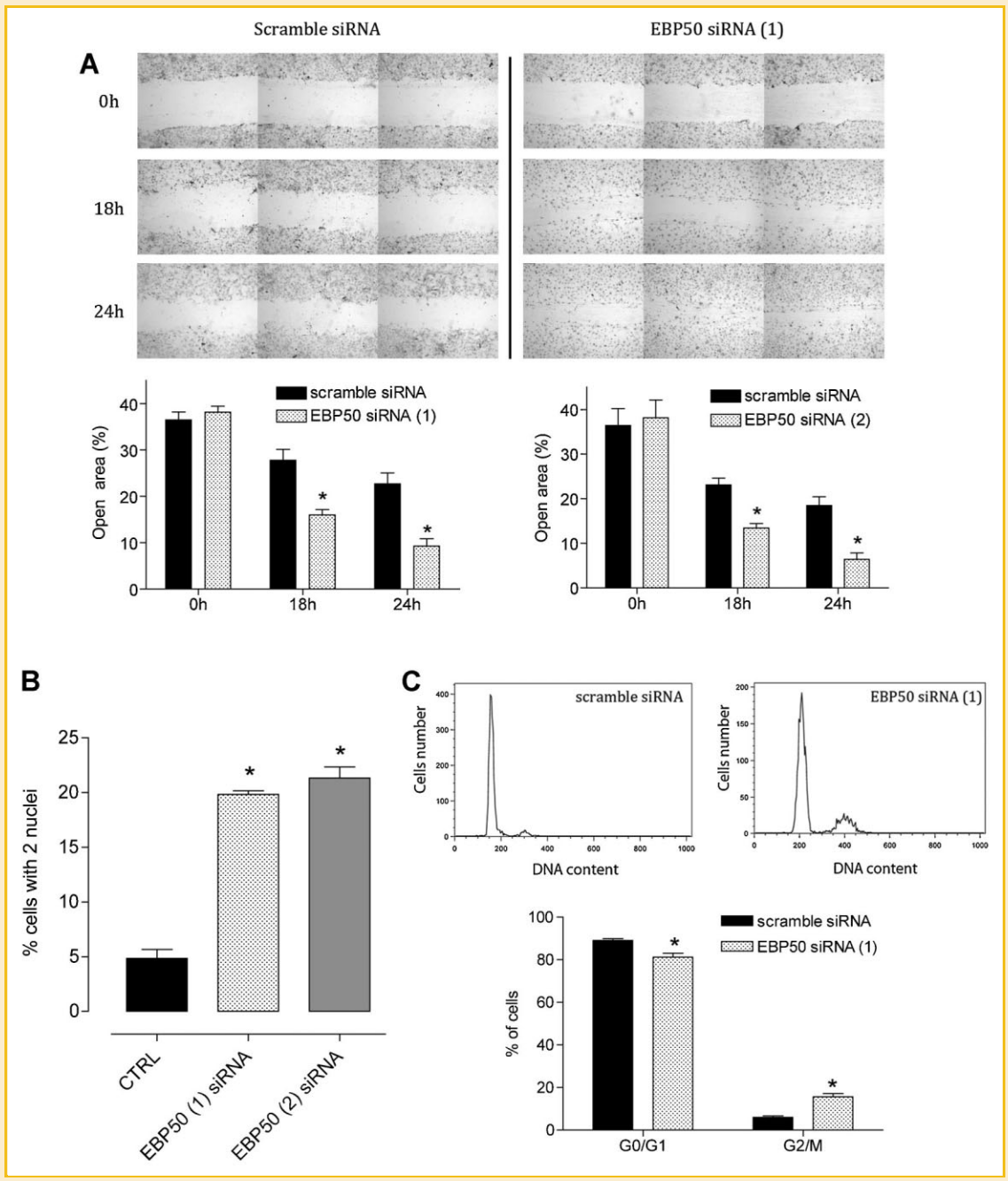

Fig. 2. Knock-down of EBP50 promotes cell migration and impairs cytokinesis. A: *Upper panels*: Representative images of cell migration after wound healing. Cells were transfected with scramble or anti-EBP50 siRNA and serum starved for 24 h before the test. *Lower panels*: Mean values of wound area expressed as percentage of total image area after 0, 18, and 24 h of cell migration (mean ± SEM, n = 8 independent experiments for anti-EBP50 siRNA #1 and n = 5 independent experiments for anti-EBP50 siRNA #2, $^{*}P < 0.05$ versus scramble siRNA transfected cells). B: Histogram represents the mean values of the proportions of binucleated cells in cultures transfected with two different anti-EBP50 siRNA compared to cells transfected with a scramble siRNA (mean ± SEM, n = 4 independent experiments with at least 200 cells, $^{*}P < 0.05$ versus scramble siRNA transfected cells). C: FACS analysis of the cell cycle in cells transfected with scramble or anti-EBP50 siRNA. The x-axis represents the fluorescence of propidium iodide and the y-axis represents the number of cells. Data are summarized in the lower panel: diploid cells are in G0/G1 phase while tetraploid cells are in G2/M phase (mean ± SEM, n = 3, $^{*}P < 0.05$ versus scramble siRNA transfected cells).

membrane probing with anti-myosin IIa antibody. This is in line with the interaction of EBP50 with myosin IIa, previously shown in noradrenaline-stimulated arteries [Baeyens et al., 2010]. Interestingly, the 140 kDa band, detected in the whole protein extract was absent in the EBP50 immunoprecipitated protein extract.

In agreement with these observations, the inhibition of myosin IIa, either by myosin IIa-targeted siRNA transfection or with blebbistatin, a myosin II inhibitor that does not discriminate IIa and IIb isoforms, increased VSMC migration (Fig. 4B,C). Interestingly, blebbistatin did not enhance migration of cells transfected with a

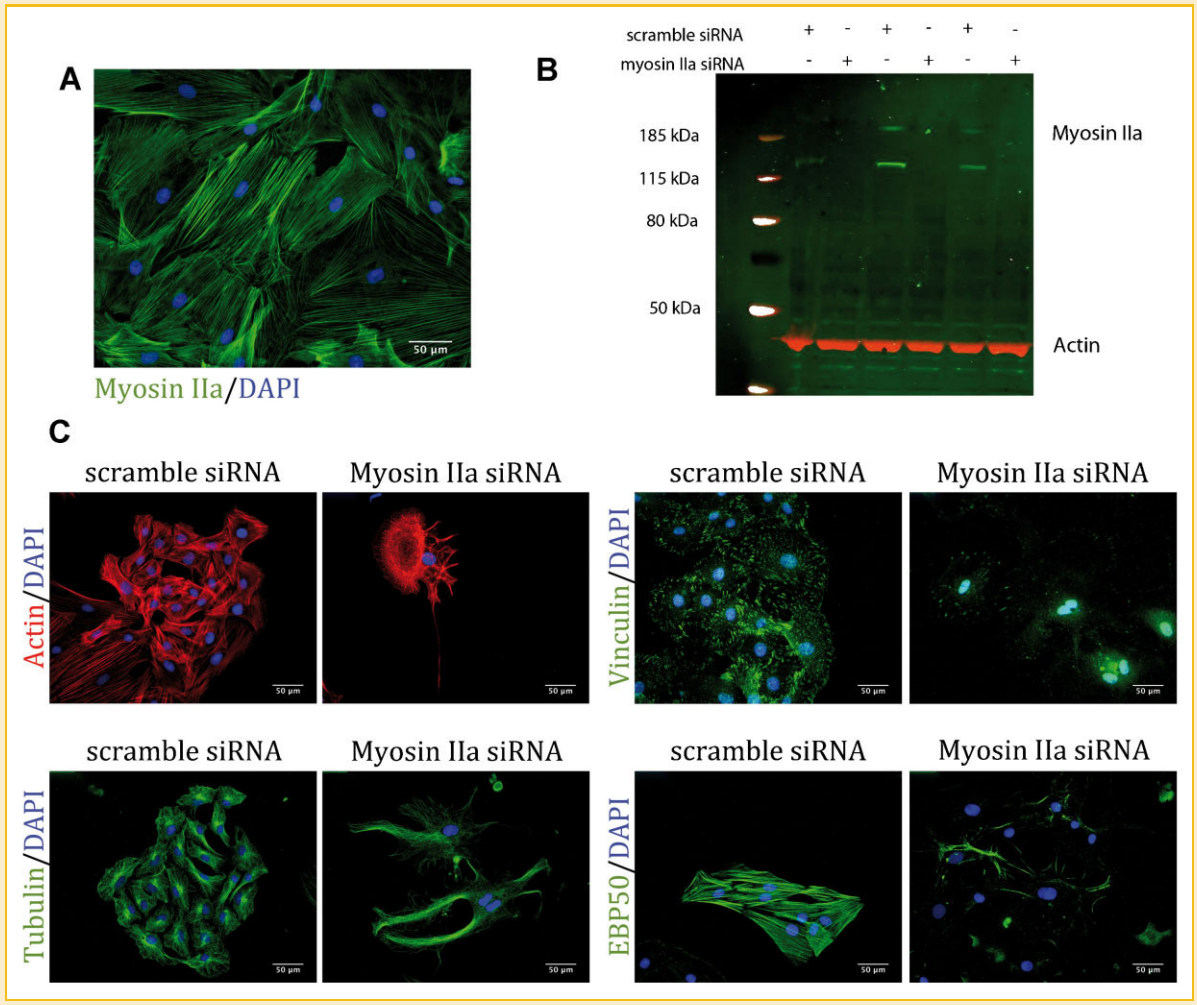

Fig. 3. Myosin IIa-depleted cells share similar architectural changes with cells depleted for EBP50. A: Immunostaining of myosin IIa (green) in VSMC. The nuclei were stained with DAPI (blue). B: Western blot of protein extracts from cells transfected for 96 h either with a scramble siRNA or an anti-myosin IIa siRNA. Membrane was immunoblotted with antibodies against myosin IIa and actin, used as loading control and IRDye conjugated secondary antibodies (680 nm for actin in red and 800 nm for myosin IIa in green). Signals were visualized and analyzed with an Odyssey infrared imager. C: Representative images of VSMC stained for F-actin, vinculin, tubulin (anti-α and -β tubulin) or EBP50 after transfection with scramble or anti-myosin IIa siRNA. Nuclei were stained with DAPI. Scale bars: 50 μm.

siRNA directed against EBP50 (Fig. 4C), indicating that inhibition of EBP50 and myosin IIa were not additive. This result suggested that EBP50 mediated its inhibitory effect on cell migration through the modulation of myosin IIa. This was confirmed by the observation that the depletion in EBP50 changed myosin IIa distribution from a fibrillar organization to a more diffuse localization (Fig. 1C). To reject the hypothesis that EBP50 depletion could affect the expression of myosin IIa, we measured the expression of myosin IIa in EBP50-depleted cells. Cell transfection with an anti-EBP50 siRNA or a scramble siRNA did not change the expression of myosin IIa (Supplemental Fig. 1).

EBP50 DEPLETION DOES NOT ACTIVATE THE PI3K PATHWAY BUT DRASTICALLY DECREASES BASAL MLC_{20} PHOSPHORYLATION LEVELS

A previous study has attributed a potential role to EBP50 in the modulation of PI3K pathway after stimulation with PDGF [Takahashi et al., 2006]. To determine whether PI3K pathway could be involved in the increased migration observed in EBP50-depleted cells, we measured Akt phosphorylation level in control cells and in cells transfected with anti-EBP50 siRNA. There was no difference in Akt phosphorylation between control and EBP50-depleted cells (Fig. 5A). As expected, PDGF-BB stimulation (20 ng/ml for 30 min) increased the phosphorylation of Akt, but the level of phosphorylated Akt was not different in control and EBP50-depleted cells. This indicates that PI3K pathway is not involved in the migration process resulting from EBP50 depletion.

To further investigate the potential role of EBP50 in the modulation of myosin IIa activity, we measured MLC_{20} phosphorylation level in control cells and in cells depleted for EBP50, in the absence of stimulation. As shown in Figure 5B, depletion of EBP50 decreased the expression of total MLC_{20} ($P = 0.008$, $n = 3$) but also drastically diminished the phosphorylation level of MLC_{20} ($P = 0.002$, $n = 3$).

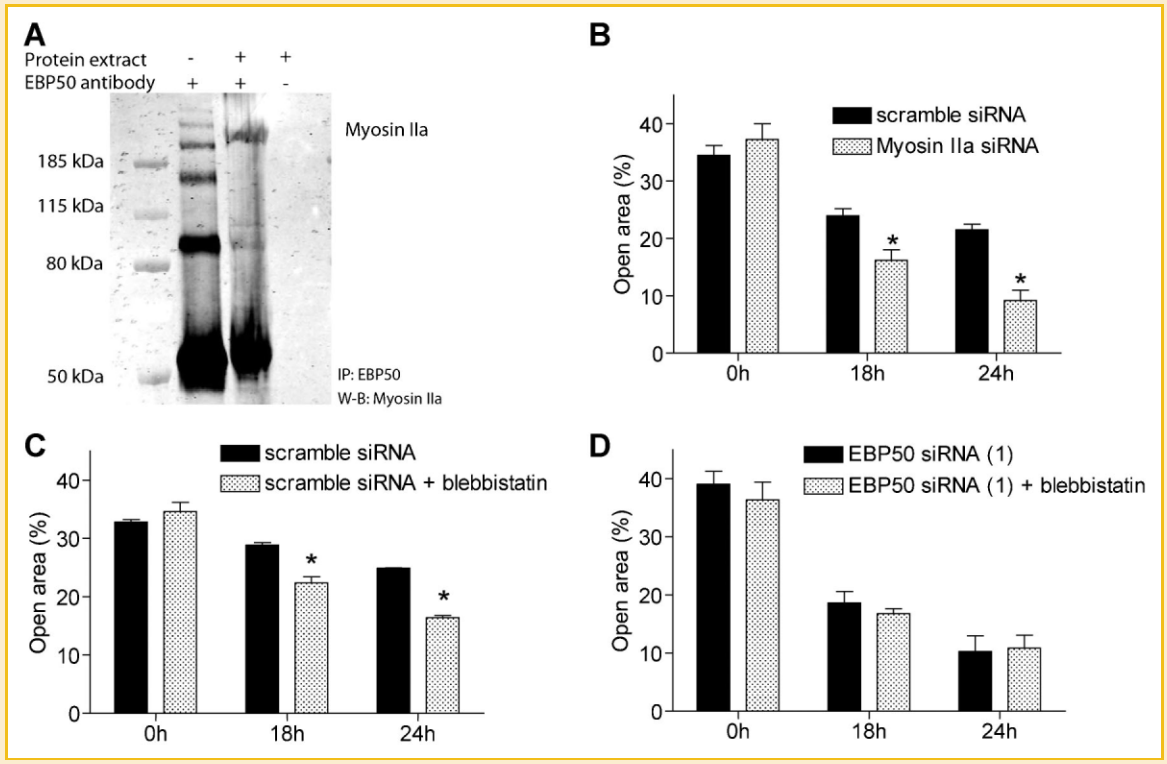

Fig. 4. EBP50 interacts with myosin IIa. A: Western blot analysis of protein extract immunoprecipitated with anti-EBP50 antibody and detected with anti-myosin IIa antibody (middle lane). Controls with antibody only without protein extract (first lane) or with protein extract incubated with sepharose beads without antibody (last lane) are shown. B: Migration analysis of cells transfected for 96 h with scramble or myosin IIa siRNA. Mean values of wound area expressed as percentage of total image area after 0, 18, and 24 h of cell migration (mean ± SEM, n = 6). C,D: Effect of blebbistatin (25 μM) on migration of cells transfected either with scramble (C) or anti-EBP50 siRNA (D) (mean ± SEM, n = 6). $^{*}P < 0.05$ versus scramble siRNA transfected cells, without blebbistatin.

EBP50 IS A LINKER BETWEEN ACTO-MYOSIN AND MICROTUBULE NETWORK

Co-immunoprecipitation revealed that EBP50 interacted with α- and β-tubulin in VSMC (Fig. 6A). The inhibition of microtubule polymerization with vinblastine blocked cell migration in control cells and impaired the enhanced cell migration evoked by EBP50 depletion (Fig. 6B), suggesting that microtubule polymerization is a major mechanism in the control of migration by EBP50.

As shown in Figures 1C and 3C, EBP50 and myosin IIa depletion drastically changed the organization of the microtubule network: there was a loss of staining around the nucleus while huge microtubule projections were visible in lamellae ruffling. To determine whether such ruffling reflected an elevated level of active Rac1 [Siegrist and Doe, 2007], we measured Rac1-GTP level in VSMC depleted in EBP50. Rac1-GTP level significantly increased in cells transfected with an anti-EBP50 siRNA compared to control cells transfected with scramble siRNA (Fig. 6C). We also observed a significant reduction in total Rac1 level in EBP50 depleted cells compared to control cells. The ratio of Rac1-GTP versus total Rac1 was markedly increased after EBP50 depletion, indicating that EBP50 is a negative regulator of Rac1 activity in VSMC.

DISCUSSION

The present study shows that EBP50 is required for the control of cell migration and cytokinesis. This important function of EBP50 is related to its contribution to the organization of myosin IIa fibers and microtubule network in VSMC.

Depletion of EBP50 in VSMC drastically changed cell morphology as shown by the decrease in actin bundles, the loss of focal adhesion, and the increase in microtubules localized in membrane lamellae. This observation is consistent with recent reports showing that EBP50 modulates cell architecture [Favia et al., 2010; Garbett et al., 2010; Hughes et al., 2010]. The particular cell architecture of EBP50-depleted cells is suggestive of a switch to a migratory phenotype characterized by the appearance of structures involved in cell migration, like lamellipodia [Etienne-Manneville, 2004; Saunders et al., 2006; Nemethova et al., 2008]. In agreement with the change in cell morphology, cells depleted for EBP50 exhibited a faster migration suggesting that EBP50 acts like a molecular brake to restrain migration. This property could be of particular importance in VSMC: in the vessel wall most VSMC have a contractile, non-migratory phenotype, but they undergo a change to a non-contractile migratory phenotype during development or under the influence of growth factors activated by pathological conditions

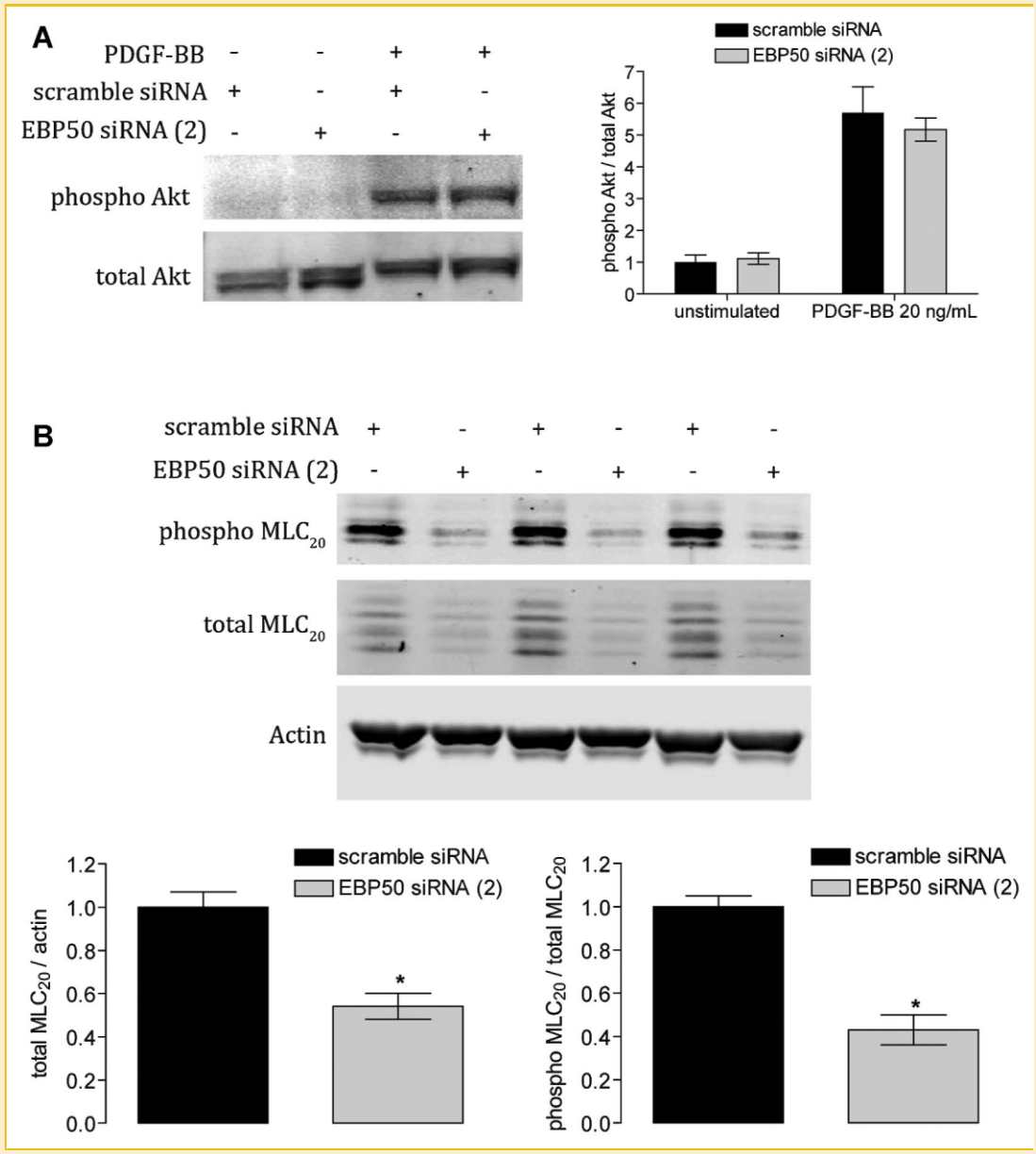

Fig. 5. EBP50 decreases basal MLC_{20} phosphorylation and does not affect Akt phosphorylation. A: Western blot of protein extracts from cells transfected with either a scramble siRNA or an anti-EBP50 siRNA. Membrane was immunoblotted with antibodies against total Akt and phospho Akt. The graph shows the ratio of phospho Akt on total Akt expression (mean ± SEM, n = 8 for unstimulated cells and n = 3 for PDGF-BB stimulated cells). B: Western blot of protein extracts from cells transfected with either a scramble siRNA or an anti-EBP50 siRNA. Membrane was immunoblotted with antibodies against total MLC_{20}, phospho MLC_{20}, and actin. The graphs show the ratio of total MLC_{20} expression on actin expression (left, mean ± SEM, n = 3, $^*P = 0.007$) and the ratio of phospho MLC_{20} on total MLC_{20} expression (right, mean ± SEM, n = 3, $^*P = 0.002$).

like atherosclerosis or post-injury stenosis. Further studies should determine the contribution of EBP50 in the pathogenesis of these vascular diseases.

Another consequence of the inhibition of EBP50 expression in VSMC was the increased number of binucleated cells suggesting a marked defect in cell division. This was confirmed by FACS analysis, showing a larger proportion of cells in the G2/M phase in EBP50-depleted cells compared to control. The inhibition of cytokinesis was not associated with apoptosis. Further studies should be conducted to investigate more deeply the role of EBP50 in this cellular process.

A common feature of migration and cytokinesis, two events that were shown in the present study to be regulated by EBP50, is the contribution of myosin IIa. Myosin IIa (encoded by the *MYH9* gene) is a member of the myosin II family, which also includes skeletal, cardiac, and smooth muscle isoforms. Recent studies have reported the inhibitory role of myosin IIa in cell migration [Katsumi et al., 2002; Even-Ram et al., 2007; Vicente-Manzanares et al., 2007; Conti and Adelstein, 2008; Lee et al., 2010; Pasapera et al., 2010]. Cytokinesis is impaired by the pharmacological inhibition of myosin IIa with blebbistatin [Straight et al., 2003] and requires the

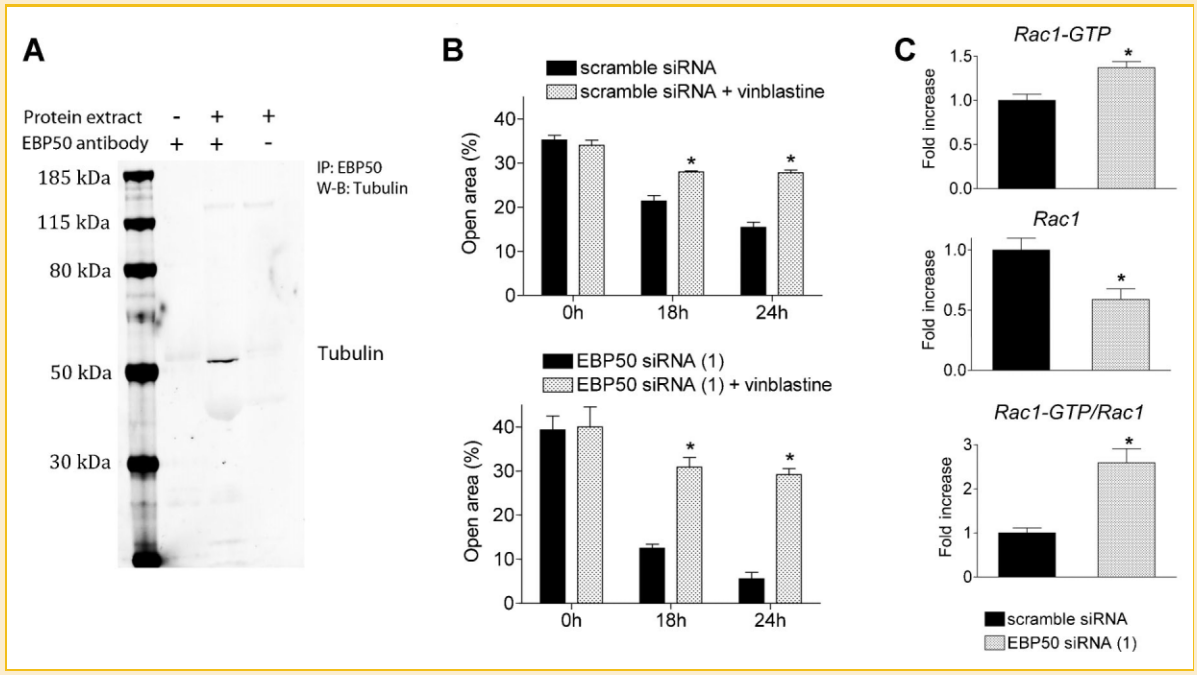

Fig. 6. EBP50 interacts with tubulin and activates Rac1. A: Western blot analysis of protein extracts immunoprecipitated with anti-EBP50 antibody and detected with anti-α and -β tubulin antibody (middle lane). Controls with antibody only without protein extract (first lane) or with protein extract incubated with sepharose beads without antibody (last lane) are shown. B: Effect of vinblastine (100 nM) on migration of cells transfected either with scramble or anti-EBP50 siRNA (mean ± SEM, n = 3). C: Rac1 activation levels quantified by measuring Rac1-GTP levels in cells transfected with scramble or EBP50 siRNA. Total Rac1 protein levels were also measured after Western blotting to allow normalization of Rac1-GTP with regard to total protein levels. Data were normalized to scramble siRNA transfected cells and expressed as mean ± SEM (n = 6) $^{*}P < 0.05$ versus scramble siRNA transfected cells.

coordinated positioning of myosin IIa contractile ring and microtubule at cleavage furrow [Barr and Gruneberg, 2007].

We have detected the expression of alternative spliced isoforms of myosin IIa in VSMC. Although theoretically alternative-spliced variants of myosin IIa could exist, no experimental evidence has been published so far [Li et al., 2008; Vicente-Manzanares et al., 2009]. The consequence of myosin IIa depletion on VSMC morphology was similar to what has been described in other cell types [Even-Ram et al., 2007; Pasapera et al., 2010], and, interestingly, was similar to the changes induced by the depletion of EBP50. In addition, the inhibition of EBP50 expression led to the disassembly of myosin IIa fibers, while myosin IIa expression was not affected, suggesting that EBP50 could help to maintain the myosin IIa organization that is required for the control of migration. This was confirmed by the observation that the inhibition of myosin IIa with blebbistatin did not affect migration of cells depleted for EBP50. We have also observed a decrease in the phosphorylation level of MLC_{20} in unstimulated EBP50-depleted cells compared to control cells, which is consistent with the disassembly of myosin IIa fibers observed in EBP50-depleted cells [Watanabe et al., 2007]. The interaction of EBP50 with myosin IIa in VSMC was demonstrated by co-immunoprecipitation, in agreement with the identification of myosin IIa as a binding partner of EBP50 in intact mesenteric artery [Baeyens et al., 2010]. However, only one alternative spliced isoform of myosin IIa was detected in proteins immunoprecipitated with EBP50 in VSMC.

The inhibition of EBP50 expression also induced a profound change in the organization of the microtubule network, which shifted from the perinuclear region to the lamellae expansions. Microtubules are essential players in the regulation of cell contraction [Cai et al., 2010], polarization [Slattum et al., 2009], migration [Even-Ram et al., 2007], and cytokinesis [Vale et al., 2009].

The interaction of EBP50 and tubulin has already been documented in airway epithelial cell line and in intact mesenteric artery [Auerbach and Liedtke, 2007; Baeyens et al., 2010] but the physiological function of this interaction was unknown. It was confirmed in VSMC, where the simultaneous binding of EBP50 to tubulin and myosin IIa suggests that EBP50 could be a linker between acto-myosin and microtubule networks. The inhibition of EBP50 expression could affect cytokinesis by disturbing the formation or the positioning of the myosin IIa ring following the disorganization of myosin IIa and/or the alteration of its interaction with the microtubule furrow. Further specific studies would be required to precisely determine the mechanism of EBP50 action.

The depletion of EBP50 or myosin IIa increased cell migration and promoted microtubule polymerization. Microtubule polymerization is required for Rac1 activation by its GEFs [Waterman-Storer et al., 1999], leading to cell migration through the reorganization of actin stress fibers and the formation of lamellipodia [Ridley and Hall, 1992; Ridley et al., 1992]. Interestingly, myosin IIa inhibition increases the level of active Rac1 [Even-Ram et al., 2007; Lee et al.,

2010]. Activation of Rac1 has been shown to result from the release of myosin-bound GEFs after the disassembly of myosin filaments [Conti and Adelstein, 2008; Lee et al., 2010], and is also described after inhibition of myosin phosphorylation and cell tension [Katsumi et al., 2002].

The present results indicated that EBP50 depletion resulted in increased Rac1 activation, suggesting that the disorganization of the microtubule–myosin IIa network after EBP50 depletion could lead to microtubule polymerization, Rac1 activation, formation of lamellipodia, and then cell migration.

In conclusion, the present results suggest that EBP50 could act as a molecular brake that links acto-myosin and the microtubule networks to control their distribution within the cell. EBP50 could be involved in the coupling between the myosin IIa contractile ring and microtubule in the cleavage furrow during cytokinesis. Depletion of EBP50 dismantles myosin IIa fibers and induces the formation of stable microtubules in lamellae expansions and Rac1 activation, leading to the formation of lamellipodia, trailing tails, and decrease of focal adhesion formation. These disturbances alter cell cytokinesis and trigger cell migration.

ACKNOWLEDGMENTS

The authors thank Prof. P. Courtoy, P. Gailly, and J. Lebacq for helpful discussion and I. Latrache for excellent technical assistance. This work was supported by grants from the Ministère de l'Education et de la Recherche Scientifique of the Belgian French Community (Action Concertée no. 06/11-339) and the Fonds pour la Recherche Scientifique Médicale. N.B. and C.dM. were supported by a fellowship from the Fund for training in Research in Industry and Agriculture.

REFERENCES

Auerbach M, Liedtke CM. 2007. Role of the scaffold protein RACK1 in apical expression of CFTR. Am J Physiol Cell Physiol 293:C294–C304.

Baeyens N, Horman S, Vertommen D, Rider M, Morel N. 2010. Identification and functional implication of a Rho kinase-dependent moesin-EBP50 interaction in noradrenaline-stimulated artery. Am J Physiol Cell Physiol 299:C1530–C1540.

Barr FA, Gruneberg U. 2007. Cytokinesis: Placing and making the final cut. Cell 131:847–860.

Cai Y, Rossier O, Gauthier NC, Biais N, Fardin MA, Zhang X, Miller LW, Ladoux B, Cornish VW, Sheetz MP. 2010. Cytoskeletal coherence requires myosin-IIA contractility. J Cell Sci 123:413–423.

Cao TT, Deacon HW, Reczek D, Bretscher A, von Zastrow M. 1999. A kinase-regulated PDZ-domain interaction controls endocytic sorting of the beta2-adrenergic receptor. Nature 401:286–290.

Choi CK, Vicente-Manzanares M, Zareno J, Whitmore LA, Mogilner A, Horwitz AR. 2008. Actin and alpha-actinin orchestrate the assembly and maturation of nascent adhesions in a myosin II motor-independent manner. Nat Cell Biol 10:1039–1050.

Conti MA, Adelstein RS. 2008. Nonmuscle myosin II moves in new directions. J Cell Sci 121:11–18.

Etienne-Manneville S. 2004. Actin and microtubules in cell motility: Which one is in control? Traffic 5:470–477.

Etienne-Manneville S, Hall A. 2002. Rho GTPases in cell biology. Nature 420:629–635.

Even-Ram S, Doyle AD, Conti MA, Matsumoto K, Adelstein RS, Yamada KM. 2007. Myosin IIA regulates cell motility and actomyosin-microtubule crosstalk. Nat Cell Biol 9:299–309.

Favia M, Guerra L, Fanelli T, Cardone RA, Monterisi S, Di Sole F, Castellani S, Chen M, Seidler U, Reshkin SJ, Conese M, Casavola V. 2010. Na+/H+ exchanger regulatory factor 1 overexpression-dependent increase of cytoskeleton organization is fundamental in the rescue of F508del cystic fibrosis transmembrane conductance regulator in human airway CFBE41o cells. Mol Biol Cell 21:73–86.

Garbett D, LaLonde DP, Bretscher A. 2010. The scaffolding protein EBP50 regulates microvillar assembly in a phosphorylation-dependent manner. J Cell Biol 191:397–413.

Gardel ML, Sabass B, Ji L, Danuser G, Schwarz US, Waterman CM. 2008. Traction stress in focal adhesions correlates biphasically with actin retrograde flow speed. J Cell Biol 183:999–1005.

Geback T, Schulz MM, Koumoutsakos P, Detmar M. 2009. TScratch: A novel and simple software tool for automated analysis of monolayer wound healing assays. Biotechniques 46:265–274.

Gerthoffer WT. 2007. Mechanisms of vascular smooth muscle cell migration. Circ Res 100:607–621.

Hughes SC, Formstecher E, Fehon RG. 2010. Sip1, the Drosophila orthologue of EBP50/NHERF1, functions with the sterile 20 family kinase Slik to regulate moesin activity. J Cell Sci 123:1099–1107.

Katsumi A, Milanini J, Kiosses WB, del Pozo MA, Kaunas R, Chien S, Hahn KM, Schwartz MA. 2002. Effects of cell tension on the small GTPase Rac. J Cell Biol 158:153–164.

Lee CS, Choi CK, Shin EY, Schwartz MA, Kim EG. 2010. Myosin II directly binds and inhibits Dbl family guanine nucleotide exchange factors: A possible link to Rho family GTPases. J Cell Biol 190:663–674.

Li Y, Lalwani AK, Mhatre AN. 2008. Alternative splice variants of MYH9. DNA Cell Biol 27:117–125.

Nemethova M, Auinger S, Small JV. 2008. Building the actin cytoskeleton: Filopodia contribute to the construction of contractile bundles in the lamella. J Cell Biol 180:1233–1244.

Pasapera AM, Schneider IC, Rericha E, Schlaepfer DD, Waterman CM. 2010. Myosin II activity regulates vinculin recruitment to focal adhesions through FAK-mediated paxillin phosphorylation. J Cell Biol 188:877–890.

Reczek D, Berryman M, Bretscher A. 1997. Identification of EBP50: A PDZ-containing phosphoprotein that associates with members of the ezrin–radixin–moesin family. J Cell Biol 139:169–179.

Ridley AJ, Hall A. 1992. The small GTP-binding protein rho regulates the assembly of focal adhesions and actin stress fibers in response to growth factors. Cell 70:389–399.

Ridley AJ, Paterson HF, Johnston CL, Diekmann D, Hall A. 1992. The small GTP-binding protein rac regulates growth factor-induced membrane ruffling. Cell 70:401–410.

Saunders RM, Holt MR, Jennings L, Sutton DH, Barsukov IL, Bobkov A, Liddington RC, Adamson EA, Dunn GA, Critchley DR. 2006. Role of vinculin in regulating focal adhesion turnover. Eur J Cell Biol 85:487–500.

Short DB, Trotter KW, Reczek D, Kreda SM, Bretscher A, Boucher RC, Stutts MJ, Milgram SL. 1998. An apical PDZ protein anchors the cystic fibrosis transmembrane conductance regulator to the cytoskeleton. J Biol Chem 273:19797–19801.

Siegrist SE, Doe CQ. 2007. Microtubule-induced cortical cell polarity. Genes Dev 21:483–496.

Slattum G, McGee KM, Rosenblatt J. 2009. P115 RhoGEF and microtubules decide the direction apoptotic cells extrude from an epithelium. J Cell Biol 186:693–702.

Song GJ, Barrick S, Leslie KL, Sicari B, Fiaschi-Taesch NM, Bisello A. 2010. EBP50 inhibits the anti-mitogenic action of the parathyroid hormone type 1 receptor in vascular smooth muscle cells. J Mol Cell Cardiol 49:1012–1021.

Straight AF, Cheung A, Limouze J, Chen I, Westwood NJ, Sellers JR, Mitchison TJ. 2003. Dissecting temporal and spatial control of cytokinesis with a myosin II Inhibitor. Science 299:1743–1747.

Takahashi Y, Morales FC, Kreimann EL, Georgescu MM. 2006. PTEN tumor suppressor associates with NHERF proteins to attenuate PDGF receptor signaling. EMBO J 25:910–920.

Vale RD, Spudich JA, Griffis ER. 2009. Dynamics of myosin, microtubules, and Kinesin-6 at the cortex during cytokinesis in Drosophila S2cells. J Cell Biol 186:727–738.

Vicente-Manzanares M, Zareno J, Whitmore L, Choi CK, Horwitz AF. 2007. Regulation of protrusion, adhesion dynamics, and polarity by myosins IIA and IIB in migrating cells. J Cell Biol 176:573–580.

Vicente-Manzanares M, Ma X, Adelstein RS, Horwitz AR. 2009. Non-muscle myosin II takes centre stage in cell adhesion and migration. Nat Rev Mol Cell Biol 10:778–790.

Watanabe T, Hosoya H, Yonemura S. 2007. Regulation of myosin II dynamics by phosphorylation and dephosphorylation of its light chain in epithelial cells. Mol Biol Cell 18:605–616.

Waterman-Storer CM, Worthylake RA, Liu BP, Burridge K, Salmon ED. 1999. Microtubule growth activates Rac1 to promote lamellipodial protrusion in fibroblasts. Nat Cell Biol 1:45–50.

Weinman EJ, Steplock D, Wang Y, Shenolikar S. 1995. Characterization of a protein cofactor that mediates protein kinase A regulation of the renal brush border membrane Na(+)-H+ exchanger. J Clin Invest 95:2143–2149.